

Supporting Information

Click Modification of a Metal-Organic Framework for Two-photon Photodynamic Therapy with Near-Infrared Excitation

Bo Li,^{†,a} Hongzhi Cao,^{†,b} Jun Zheng,^a Bo Ni,^c Xin Lu,^c Xiaohe Tian,^b Yupeng Tian^c and Dandan Li^{*,a}

^aInstitutes of Physical Science and Information Technology, Key Laboratory of Structure and Functional Regulation of Hybrid Materials, Ministry of Education, Anhui University, Hefei 230601 (China).

^bSchool of Life Science, Anhui University, Hefei 230601 (China).

^cCollege of Chemistry and Chemical Engineering, Anhui University, Hefei 230601 (China).

[†]These authors contributed equally to this work.

*To whom correspondence should be addressed.

E-mail: chemlidd@163.com.

Table of Contents

1 Experimental and methods.....	5
1.1 Materials and apparatus	5
1.2 Two-photon excited fluorescence (2PEF) spectroscopy and two-photon absorption (2PA) cross-section	5
1.3 ROS-generation detection.....	5
1.4 Singlet oxygen ($^1\text{O}_2$) generation detection.....	5
1.5 Singlet oxygen quantum yield (Φ_s)	6
1.6 Superoxide anion radical ($\text{O}_2^{\bullet-}$) detection.	6
1.7 Electron spin resonance (ESR) assay.....	6
1.8 Cell culture.....	6
1.9 Culture of 3D multicellular tumor spheroids (3D MCTs)	7
1.10 Cell uptake analysis	7
1.11 Cytotoxicity assays in cells.....	7
1.12 The one/two-photon fluorescence imaging study of PCN-58-Ps-HA	8
1.13 ROS generation under two-photon laser in vitro	8
1.14 Live/Dead assay with calcein AM/PI	8
1.15 The pharmacokinetic of PCN-58-Ps-HA	8
1.16 The discussion on the scalable and feasible of the production for PCN-58-Ps-HA	8
2 Supporting Schemes and Figures.....	9
2.1 Synthesis of TPDC-2CH₂N₃	9
2.2 Synthesis of (<i>E</i>)-2-(4-(diethylamino) styryl)-3-(prop-2-yn-1-yl)benzo[<i>d</i>]thiazol-3-ium bromide (Ps)	12
Figure S7 SEM images of PCN-58 synthesized in 10 mL glass bottles (a), 25 mL glass bottles (b) and 50 mL glass bottles (c).	14

Figure S8 a) TEM image of PCN-58 . b) SEM image of PCN-58 . c) TEM image of PCN-58-Ps . d) SEM image of PCN-58-Ps	14
Figure S9 DLS measurement of PCN-58 (a), PCN-58-Ps (b) and PCN-58-Ps-HA (c).	14
Figure S10 The morphology of PCN-58-Ps-HA in deionized water solution at different time.	14
Figure S11 Dispersion photo of PCN-58-Ps-HA and PCN-58-Ps in aqueous solution.	15
Figure S12 Photo of Ps and PCN-58-Ps-HA without UV lamp exposure.	15
Figure S13 Quantitative fluorescence yield of PCN-58-Ps (a) and Ps (b).	15
Figure S14 a) Two-photon excited luminescence of PCN-58-Ps-HA with femtosecond laser excitation at 910 nm with different input power. b) Two-photon absorption verification of PCN-58-Ps-HA . c) Two-photon excited spectrum of Ps from 870 nm to 970 nm. d) Two-photon excited luminescence of Ps with femtosecond laser excitation at 900 nm with different input power. (Inset: two-photon absorption verification of Ps).	16
Figure S15 Emission spectra of PCN-58-Ps-HA in the solution of DCFH under laser irradiation with different time.	16
Figure S16 The fluorescence intensity of DHR123 at 525 nm after the LED light (400 - 700 nm, 40 mW/cm ²) irradiation for 150s in DHR123 Only, Ps , PCN-58-HA and PCN-58-Ps-HA solution. In contrast to the negligible changes of Ps , the evidently enhanced emission of DHR 123 sensitized by PCN-58-HA and PCN-58-Ps-HA confirmed the light-induced O ₂ ^{•-} generation ability of PCN-58	17
Figure S17 a) CLSM images of Hela cells incubated with PCN-58-Ps-HA and control group (PCN-58-Ps-HA treated with free HA in advance). b) Quantitative detection of intracellular fluorescence intensity of PCN-58-Ps-HA	17
Figure S18 Cell viability of HepG2 cells treated with PCN-58-Ps-HA at different concentration with (blue) and without (red) NIR, indicating the good biocompatibility of PCN-58-Ps-HA at even high concentration.	17
Figure S19 CLSM images of HeLa cells after different treatments and then irradiated for 30 min, stained with calcein AM/PI (910 nm, 0.2 W/cm ²).	18
Figure S20 a) One-photon (561 nm, 0.2 W/cm ²) and b) two-photon (910 nm, 0.2 W/cm ²) fluorescence images of tissue section incubated with PCN-58-Ps-HA with different penetration depth along the z axis.	18
Figure S21 a) Two-photon CLSM images (910 nm, 0.2 W/cm ²) of Hela cells treated with PCN-58-Ps-HA and detect the generation of ¹ O ₂ and O ₂ ^{•-} using SOSG, DHE as the ¹ O ₂ , O ₂ ^{•-} fluorescence indicator, respectively. Victim C, an inhibitor with ROS. b) Fluorescence intensity of SOSG and DHE in Hela cells treated with PCN-58-Ps-HA . c) Annexin V-FITC / PI were indicator of apoptosis.	19
Figure S22 Blood circulation curve of PCN-58-Ps-HA determined by measuring the Zr	19

Table S1 Elemental analysis of PCN-58 and PCN-58-Ps-HA	20
Table S2 Zr content in Hela cells determined by ICP-MS.....	20
References	21

1 Experimental and methods

1.1 Materials and apparatus

The general chemicals were obtained from Shanghai Energy Chemical (China) and Macklin (China). Annexin V-FITC/PI Apoptosis Detection Kit were obtained from Shanghai Bestbio (China). The ^1H -NMR and ^{13}C -NMR spectra were recorded on at 25 °C, using Bruker 400/600 Ultra shield spectrometer were reported as parts per million (ppm) from TMS (δ). ESI Mass Spectrometer was recorded using LTQ Orbitrap XL. UV-vis absorption spectra were recorded on a UV-265 spectrophotometer. SEM were detected by REGULUS8230*. TEM were carried on a JEM-2100. XRD were recorded on SmartLab 9KW. Fluorescence measurements were carried out on a Hitachi F-7000 fluorescence spectrophotometer. IR spectra were recorded on a Nicolet FT-IR instrument (mid-IR: 4000 ~ 400 cm^{-1} range with KBr discs). Quantum yield was determined by FLUORMAX-4P. Element analysis were recorded on Vario EL-3. One- and two-photon imaging data acquisition and processing were performed using Lecia TCS SP8 DIVE FALCON which equipped with single-wavelength laser (output wavelength: 405 nm, 456 nm, 488 nm, 514 nm, 561 nm, 633 nm) and femtosecond laser (adjustable output wavelength: 680 - 1080 nm, 80 MHz, 140 fs). ICP-MS measurements were performed on a Thermo SCIENTIFIC iCAP Q.

1.2 Two-photon excited fluorescence (2PEF) spectroscopy and two-photon absorption (2PA) cross-section

2PEF spectra were obtained by the two-photon excited fluorescence (2PEF) method with a femtosecond laser pulse and a Ti: sapphire system (680 - 1080 nm, 80 MHz, 140 fs) as the light source. The reference sample is Rhodamine B with a concentration of 1.0×10^{-3} M. The concentration of **Ps** was 1.0×10^{-3} M. The concentration of **PCN-58-Ps-HA** was 1 mg/mL. 2PA cross section was calculated by using the following equation:

$$\delta = \delta_{ref} \frac{\Phi_{ref}}{\Phi} \frac{c_{ref}}{c} \frac{n_{ref}}{n} \frac{F}{F_{ref}}$$

Here, ref stand for reference sample, δ is the two-photon absorption cross section, Φ is two-photon quantum yield, c is the concentration of the sample, n is refractive index, F is two-photon fluorescence integral area. The absolute value of the two-photon absorption cross section of the reference sample is derived from the literature.¹

1.3 ROS-generation detection

DCFH was used as the ROS-monitoring agent. 20 μL of DCFH stock solution (1.0 mM) and 100 μL of **PCN-58-Ps-HA** (1 mg/mL) were added to 2 mL PBS solution, and LED light (400 - 700 nm, 40 mW/cm^2) was employed as the light source. The emission of DCFH at 525 nm was recorded under various irradiation times.²⁻³

1.4 Singlet oxygen ($^1\text{O}_2$) generation detection

The singlet oxygen was measured by a singlet oxygen indicator named 1,3-Diphenylisobenzofuran (DPBF). Briefly, 2 mL of DI water solution was mixed with **PCN-58-Ps-HA/PCN-58-HA** (50 µg/mL)/**Ps** (10 µM) and DPBF (100 µM). Then the cuvette was exposed to LED light (400 - 700 nm, 40 mW/cm²) irradiation for different time. The absorption spectra of DPBF at 420 ± 5 nm showed a gradual decline with the irradiation.⁴

1.5 Singlet oxygen quantum yield (Φ_s)

The relative Φ_s values of **PCN-58-Ps-HA** were measured by the standard method using DPBF as the ¹O₂ indicator and [Ru(bpy)₃]²⁺ ($\Phi_{ps} = 0.18$) as the standard in water. The air-saturated aqueous solution of **PCN-58-Ps-HA** (50 µg/mL) containing with DPBF (100 µM) was measured under irradiation and dark conditions in a time interval from 0 to 30 s. The absorption of DPBF at 420 ± 5 nm was recorded by a UV-vis spectrophotometer. The Φ_{ps} values were calculated by means of the variation of absorption spectra of DPBF at 420 ± 5 nm with the following equation:

$$\Phi_s(PS) = \Phi_{s(std)} \times \left(\frac{S_{PS}}{S_{std}} \right) \times \left(\frac{F_{std}}{F_{PS}} \right)$$

where PS designates **PCN-58-Ps-HA**, and std designates [Ru(bpy)₃]²⁺. S represents the slope of the plot of the absorbance of DPBF. F stands for the correction factor of absorption, which equals to 1 to 10^{-OD}. (OD is the optical density of complexes and [Ru(bpy)₃]²⁺ at 556 nm).⁴

1.6 Superoxide anion radical (O₂^{•-}) detection.

Dihydrorhodamine 123 (DHR123) was used as the superoxide anion radical indicator. Both **PCN-58-Ps-HA** (50 µg/mL)/**PCN-58** (50 µg/mL)/**Ps** (10 µM) and DHR123 (100 µM) were prepared in DI water, respectively. Then the cuvette was exposed to a LED light (400 - 700 nm, 40 mW/cm²) for different time, and the fluorescence spectra was observed to rise immediately after irradiation.⁵

1.7 Electron spin resonance (ESR) assay.

ESR was used to assess the generation of ¹O₂ and O₂^{•-} by **PCN-58-Ps-HA**. The spin traps 2,2,6,6-tetramethylpiperidine (TEMP for trapping ¹O₂, 20 µL) and 5,5-dimethyl-1-pyrroline-N-oxide (DMPO for trapping O₂^{•-}, 20 µL) were used to verify the species of reactive oxygen species (ROS) generated by **PCN-58-Ps-HA** (50 µg/mL). The ESR signals of the **PCN-58-Ps-HA** (50 µg/mL) before and after LED light (400 - 700 nm, 40 mW/cm²) irradiation were recorded.⁵⁻⁶

1.8 Cell culture

The Hela cells and HepG2 cells were cultured in 25 cm² culture flasks in DMEM, supplemented with fetal bovine serum (10%), penicillin (100 units/mL) and streptomycin (50 units/mL) at 37 °C in a CO₂ incubator (95% relative humidity, 5% CO₂). Cells were seeded in 35 mm glass bottom cell culture dishes, at a density of 1 × 10⁵ cells and were allowed to grow when the cells reached more than 60% confluence. The three compounds were dissolved in DMSO with concentration of 1 mM as stock

solution, and the commercial dyes were prepared as 1 mM PBS solution and diluted to working concentration as protocol required.

1.9 Culture of 3D multicellular tumor spheroids (3D MCTs)

5 mL Poly HEMA solution was added to 25 mL cell culture flask, the ethanol was evaporated at 37 °C, and then sterilized under ultraviolet lamp for 3 - 5 h. The culture flask was washed twice with PBS, and then 1 mL mother liquor of tumor cells was added. When the cell mass density was relatively high, the flask treatment was conducted, and the cells were further cultured for 3 - 5 days, 3D multicellular spheroids could be formed with appropriate diameter.⁷ 3D MCTs were incubated with **PCN-58-Ps-HA** (50 µg/mL) for 12h. Then, 3D MCTs stained with Syto 63 and PI for 15 min, then washed with PBS solution and analyzed by confocal laser scanning microscope (CLSM).

1.10 Cell uptake analysis

Hek 293T cells (CD44-negative cells) and Hela cells (CD44-positive cells) were seeded onto corresponding cell culture dishes and grown to about 70% confluency before used. Hek 293T cells were treated with **PCN-58-Ps-HA** (50 µg/mL), Hela cells were treated with **PCN-58-Ps** (50 µg/mL) and **PCN-58-Ps-HA** (50 µg/mL), respectively. In order to further verify the cancer-specific targeting of **PCN-58-Ps-HA**, Hela cells were precultured with 10 times of HA before incubation with **PCN-58-Ps-HA**. And after 12 h incubation, the cellular uptake ability of **PCN-58-Ps-HA** were analyzed using CLSM.⁸⁻⁹ A density of 10⁵ cells per well were cultured in a 6-well plate for 24 h to allow the attachment of cells and then be applied to detect the content of Zr element in HeLa cells. After cells were washed twice by PBS (10 mM, pH = 7.4) solution, **PCN-Ps**, **PCN-58-Ps-HA** (treated with free HA in advance), and **PCN-58-Ps-HA** (300 µL, 1 mg/mL) were added to above culture medium. The cells were incubated for 12 h and then dispersed into 1mL nitric acid (65% - 68%). And then 50 µL solution was diluted into 5mL of deionized water. The concentrations of Zr element were measured by ICP-MS.

1.11 Cytotoxicity assays in cells

The study of the PDT effect of **PCN-58-Ps-HA** was carried out using the methylthiazolyldiphenyl-tetrazolium bromide (MTT) assay. **PCN-58-Ps-HA** stock solutions were diluted by fresh medium in to desired concentration (10, 25, 50, 75, 100 µg/mL). HeLa cells and HepG2 cells were cultured in a 96-well plate for 24 h before experiments. The cell medium was then exchanged by different concentrations of **PCN-58-Ps-HA** medium solutions. They were incubated at 37 °C in 5% CO₂ for 12 h before cell viability was measured by the MTT assay. The cell medium solutions were exchanged by 100 µL of fresh medium, followed by the addition of 20 µL (5 mg/mL) MTT solution to each well. The cell plates were then incubated at 37 °C in 5% CO₂ for 4 h. After MTT medium removal, the formazan crystals were dissolved in DMSO (100 µL/well) and the absorbance was measured at 490 nm using a microplate reader. And duplicated experiments have been tested.

Furthermore, the apoptosis assay of HeLa cells was assessed by flow cytometry. HeLa cells were incubated with **PCN-58-Ps-HA** (50 $\mu\text{g/mL}$) for 12 h. For the PDT group, the HeLa cells were irradiated with a LED light (400 - 700 nm, 40 mW/cm^2) for 10 and 20 min, respectively. For the dark group, the cells were incubated under dark condition. The cells were harvested and stained with Annexin V-FITC and PI for 30 min, and then washed with PBS solution and analyzed by flow cytometry.

1.12 The one/two-photon fluorescence imaging study of PCN-58-Ps-HA

A Lecia TCS SP8 DIVE FALCON which equipped with single-wavelength laser (output wavelength: 405 nm, 456 nm, 488 nm, 514 nm, 561 nm, 633 nm) and femtosecond laser (adjustable output wavelength: 680 - 1080 nm, 80 MHz, 140 fs) was employed to achieve one/two-photon fluorescence imaging. HeLa cells were treated with **PCN-58-Ps-HA** for 12h. And then, slices were prepared from cardiac muscle tissue in Balb/c mice. The tissue sections were cut to 200 μm thickness. The tissue sections were incubated with **PCN-58-Ps-HA** for 30 min. The one-photon fluorescence emission was observed from 580 to 610 nm upon excitation at 561 nm (0.2 W/cm^2). The two-photon fluorescence emission was observed from 600 to 650 nm upon excitation at 910 nm (0.2 W/cm^2).

1.13 ROS generation under two-photon laser in vitro

The ROS production in living cells was also assessed. HeLa cells were seeded in Petri dishes and incubated for 24 h. **PCN-58-Ps-HA** (50 $\mu\text{g/mL}$) in glucose-free RPMI 1640 medium was added and incubated with the cells for 12 h. Then, the cells were washed with PBS solution and incubated with SOSG (5 μM) and DHE (5 μM) for 30 min, after which the cells were incubated shielded from laser or irradiated for 5 min (910 nm laser). And then the cells were observed by CLSM.

1.14 Live/Dead assay with calcein AM/PI

HeLa cells with a density of 10^5 cells per well were cultured in a 6-well plate for 24 h to allow the attachment of cells. After cells were washed twice by PBS (10 mM, pH = 7.4) solution, **PCN-58-Ps**, **PCN-58-Ps-HA** (treated with free HA in advance), and **PCN-58-Ps-HA** (300 μL , 1 mg/mL) were added to above culture medium. The cells were incubated for 24 h, calcein AM and PI were used to confirm the viability of HeLa cells. Fluorescence images were collected by CLSM.¹⁰

1.15 The pharmacokinetic of PCN-58-Ps-HA

For pharmacokinetic of **PCN-58-Ps-HA**, female Balb/c mice ($n = 3$) were intravenous injected with **PCN-58-Ps-HA** (200 μL , 5 mg/kg). At 5 min, 20 min, 40 min, 1 h, 2 h, 4 h, 7 h, 18 h, 24 h, 48h post injection, 100 μL of blood were collected and dispersed into 1mL nitric acid (65% - 68%) to dissolve the remained **PCN-58-Ps-HA**. And then 50 μL solution was diluted into 5mL of deionized water. The concentrations of Zr element were measured by ICP-MS.¹¹⁻¹²

1.16 The discussion on the scalable and feasible of the production for PCN-58-Ps-HA

Firstly, the synthesis method of MOF holds the advantages of simple and mild preparation process, well repeatability and high yields. Upon fixing the concentration, the reaction volumes were expanded

from 10 mL to 25, 50 mL. Of note, it results in a negligible impact on the morphology (Figure S7) and yields ($\approx 70\%$).

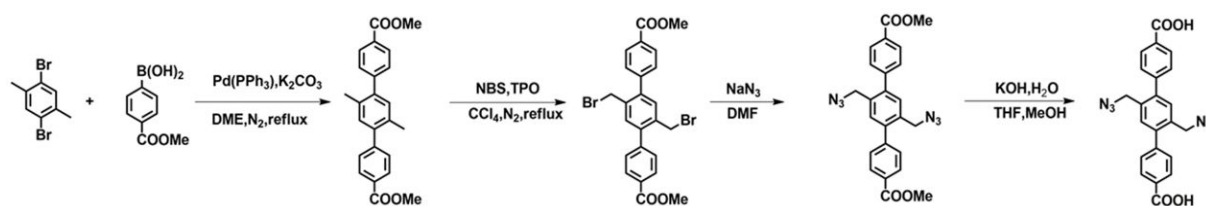
Secondly, in this work, we introduced azide - alkynyl groups for the click reaction. As reported, the involved click reaction is mild and the advantages of high selectivity and high yield.¹³⁻¹⁵

Finally, the modification of HA is simple and efficient. No additional strict temperature control required during the modification process (simple stirring method at room temperature).⁸⁻¹⁰

The above results demonstrated that the production of **PCN-58-Ps-HA** is scalable and feasible.

2 Supporting Schemes and Figures

2.1 Synthesis of TPDC-2CH₂N₃



Scheme S1 Synthetic procedures for **TPDC-2CH₂N₃**.

The 1st step: Ethylene glycol dimethyl ether (DME, 250 mL) was bubbling with nitrogen for around 1 h before introducing into nitrogen-protected solid mixture of 1,4-dibromo-2,5-dimethylbenzene (4 g, 15.2 mmol), 4-(methoxycarbonyl)phenylboronic acid (6.57 g, 36.48 mmol), potassium carbonate (12.59 g, 91.2 mmol) and tetrakis (triphenylphosphine) palladium (0.5 g, 0.43 mmol). The mixture was allowed to reflux for 3 days under nitrogen protection. After filtration, the solvent was evaporated to dryness. The residue was washed with a large amount of acetone. The residue was purified with column chromatography (silica gel, CH₂Cl₂) to give the ester as a white solid (4 g).¹⁶

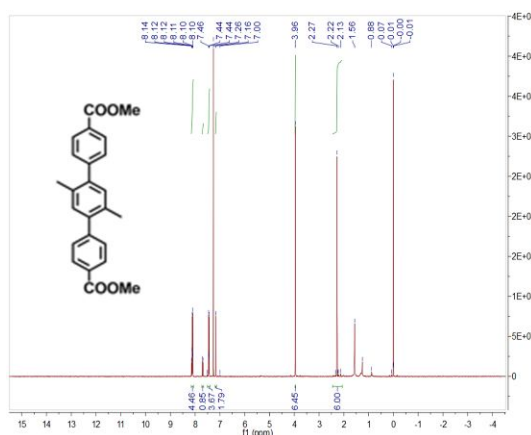


Figure S1 ¹H NMR (400 MHz, CDCl₃, r.t.) spectrum.

The 2nd step: The dimethyl ester (2.0 g, 5.35 mmol), N-Bromosuccinimide (2.0 g, 11.23 mmol), and benzoyl peroxide (120 mg) were stirred in carbon tetrachloride (50 mL) under nitrogen protection to reflux for 12-18 h. After cooling to room temperature, the solvent was removed. The residue was washed with MeOH to give benzyl bromide ester as a white solid (1.95 g).¹⁶

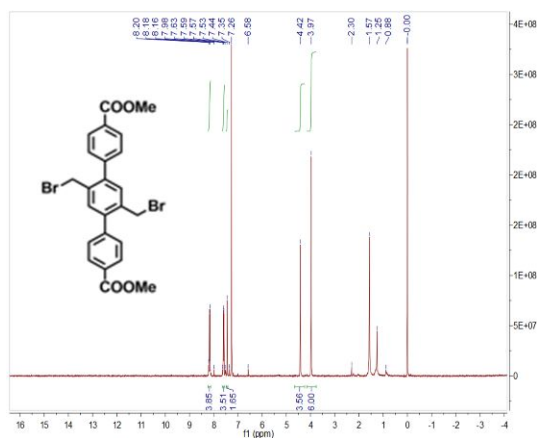


Figure S2 ^1H NMR (400 MHz, CDCl_3 , r.t.) spectrum.

The 3rd step: The benzyl bromide ester (2.0 g, 3.76 mmol) and sodium azide (2.44 g, 37.6 mmol) were stirred in DMF (60 mL) at 60-70 °C under nitrogen protection for 10-18 h. After cooling to room temperature, reaction mixture was diluted with a large amount of water. After filtration, the residue was washed with additional water to give azide ester as a light-orange solid (1.5 g).¹⁶

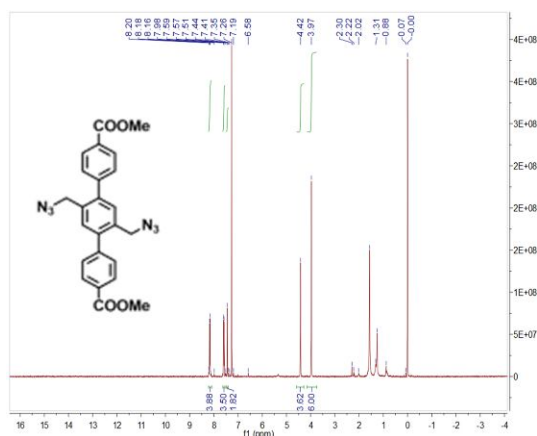
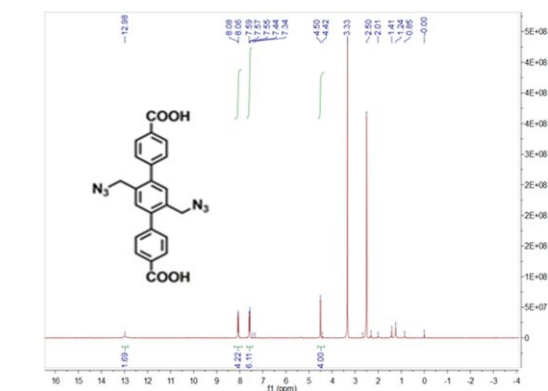
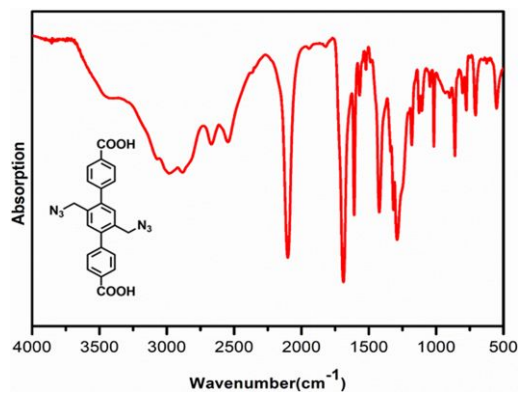


Figure S3 ^1H NMR (400 MHz, CDCl_3 , r.t.) spectrum.

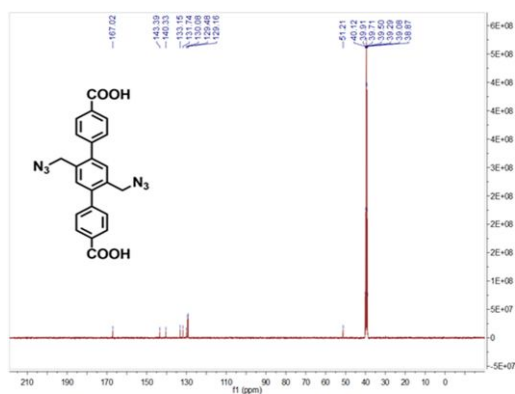
The 4th step: The azide ester (2.49 g, 5.46 mmol) was stirred in THF (80 mL) and MeOH (80 mL) mixed solvent, to which a solution of KOH (9.17 g, 163.8 mmol) in H_2O (80 mL) was introduced. This mixture was refluxed for 12 h. After cooling down to room temperature, THF and MeOH were evaporated. Additional water was added to the resulting water phase and the mixture was slightly heated until the solid was fully dissolved, then the homogeneous solution was acidified with diluted HCl until no further precipitate was detected ($\text{pH} = 2-3$). The light orange solid TPDC- $2\text{CH}_2\text{N}_3$ was collected by filtration, washing with water and drying in vacuum (2.25 g).¹⁶



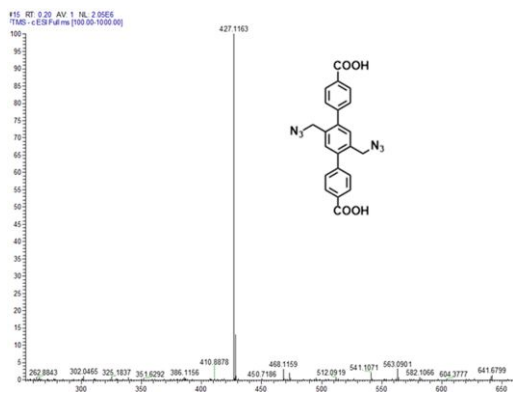
(a)



(b)



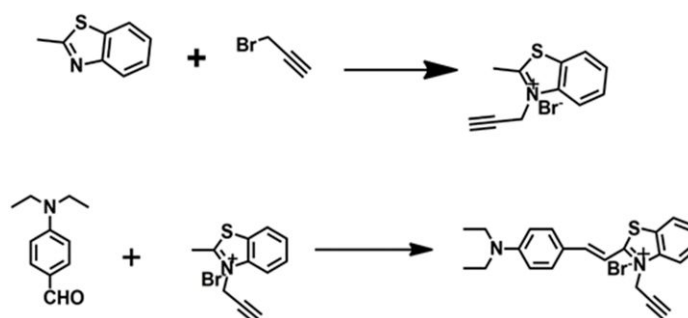
(c)



(d)

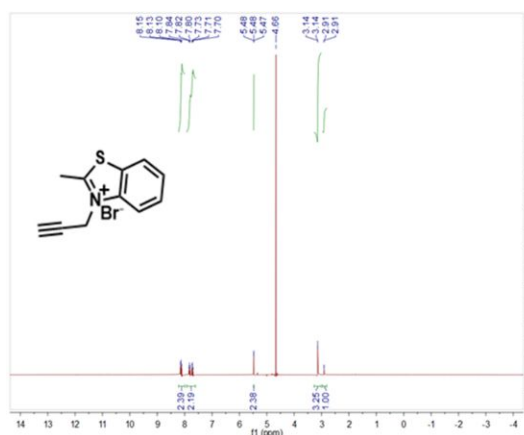
Figure S4 a) ^1H NMR (400 MHz, d_6 -DMSO, r.t.), b) IR spectrum, c) ^{13}C NMR (100 MHz, d_6 -DMSO, r.t. and d) mass spectrum of **TPDC-2CH₂N₃** ligand.

2.2 Synthesis of (*E*)-2-(4-(diethylamino) styryl)-3-(prop-2-yn-1-yl)benzo[*d*]thiazol-3-ium bromide (Ps)

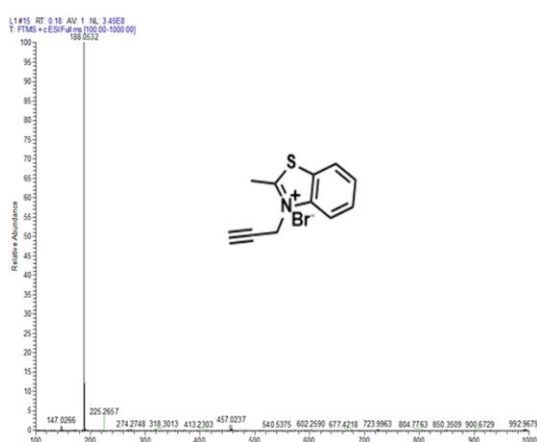


Scheme S2 Synthetic procedures for **Ps**.

Synthesis of 2-methyl-3-(prop-2-yn-1-yl)benzo[*d*]thiazol-3-ium bromide: 3-bromopropyne (7.08 g, 0.06 mol) and 2-methylbenzothiazole (10.03 g, 0.06 mol) were refluxed in 15 mL acetonitrile for 24 h. After cooling down to room temperature, the mixture was filtered to obtain residue, and the residue was washed with additional acetonitrile, then the gray solid was obtained (7.1 g).



(a)

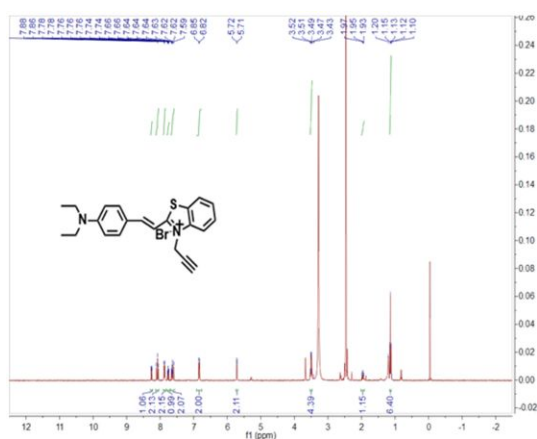


(b)

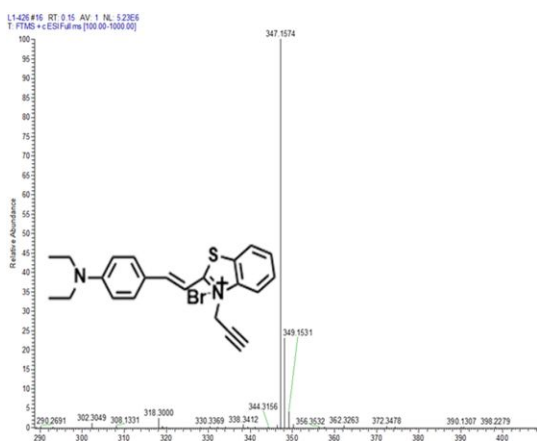
Figure S5 a) ^1H NMR (400 MHz, D_2O , r.t.) and b) mass spectrum (methanol, r.t.).

Synthesis of Ps: (*E*)-2-methyl-3-(prop-2-yn-1-yl)benzo[*d*]thiazol-3-ium bromide (2 g, 7 mmol) and 4-Diethylaminobenzaldehyde (1.33 g, 7 mmol) were stirred in ethanol (15 mL). Then three drops of piperidine were added into the mixture. The mixture was refluxed for 5 h under nitrogen protection.

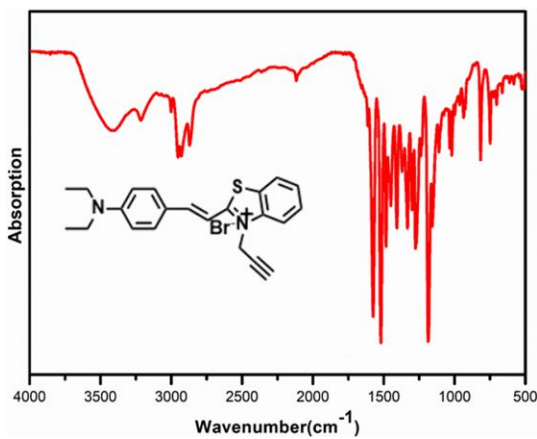
After cooling down to room temperature, the solvent was filtered to give residue, the residue was washed with additional ethanol, the purple solid was got (1.67 g).



(a)



(b)



(c)

Figure S6 a) ^1H NMR (400 MHz, d_6 -DMSO, r.t.), (b) IR spectrum and (c) mass spectrum (methanol, r.t.) of **Ps**.

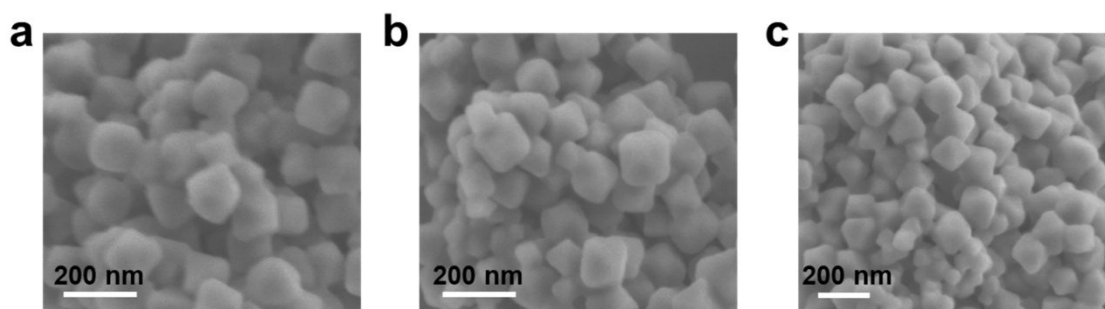


Figure S7 SEM images of **PCN-58** synthesized in 10 mL glass bottles (a), 25 mL glass bottles (b) and 50 mL glass bottles (c).

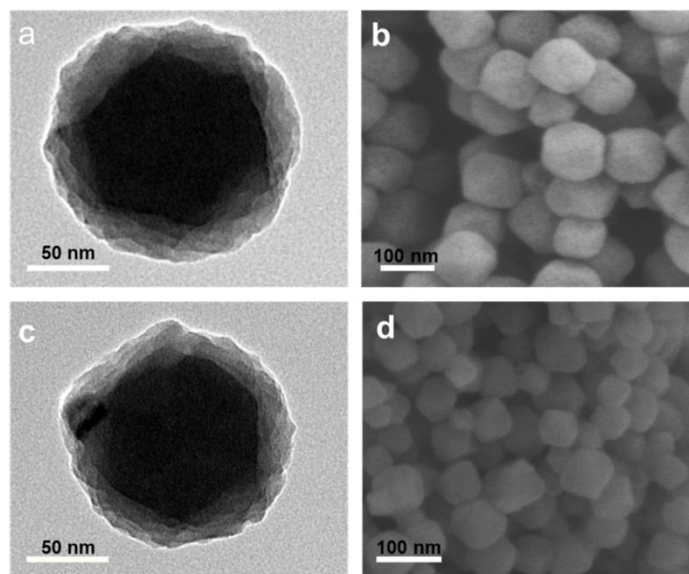


Figure S8 a) TEM image of **PCN-58**. b) SEM image of **PCN-58**. c) TEM image of **PCN-58-Ps**. d) SEM image of **PCN-58-Ps**.

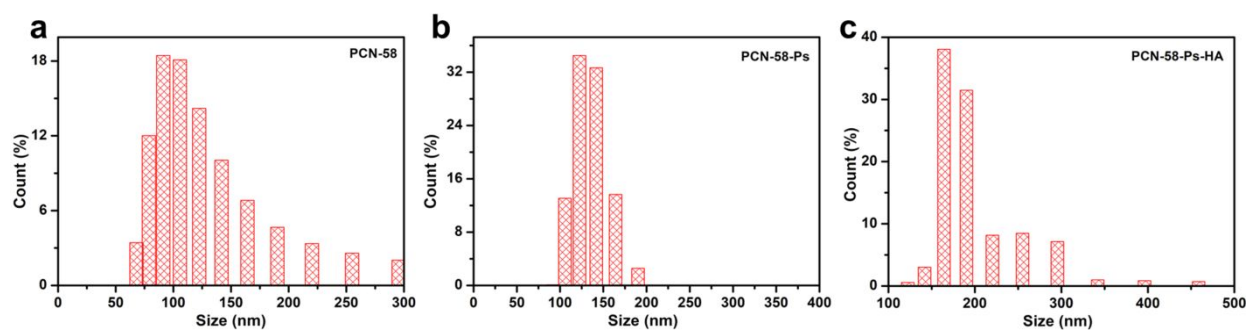


Figure S9 DLS measurement of **PCN-58** (a), **PCN-58-Ps** (b) and **PCN-58-Ps-HA** (c).

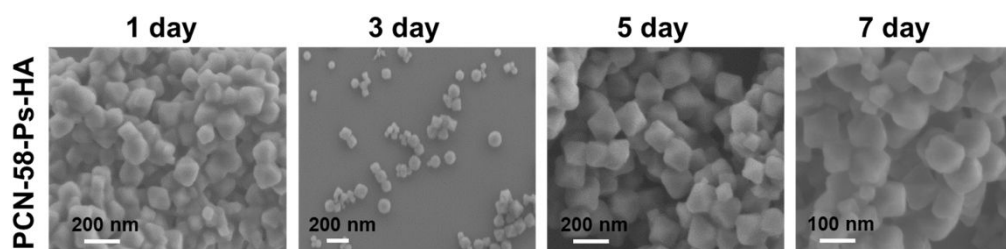


Figure S10 The morphology of **PCN-58-Ps-HA** in deionized water solution at different time.



Figure S11 Dispersion photo of PCN-58-Ps-HA and PCN-58-Ps in aqueous solution.

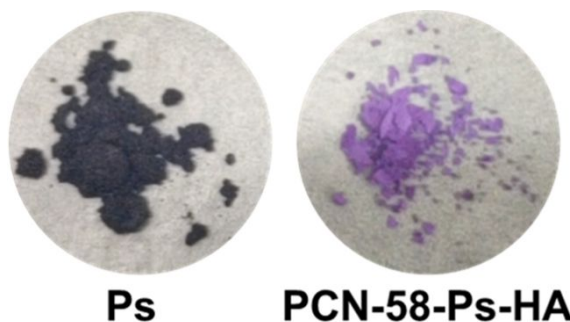


Figure S12 Photo of Ps and PCN-58-Ps-HA without UV lamp exposure.

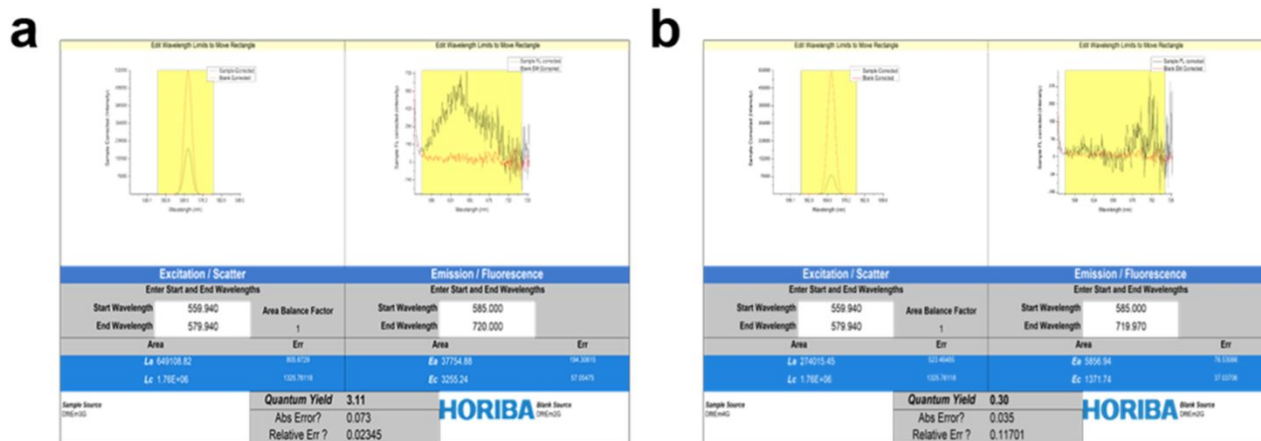


Figure S13 Quantitative fluorescence yield of PCN-58-Ps (a) and Ps (b).

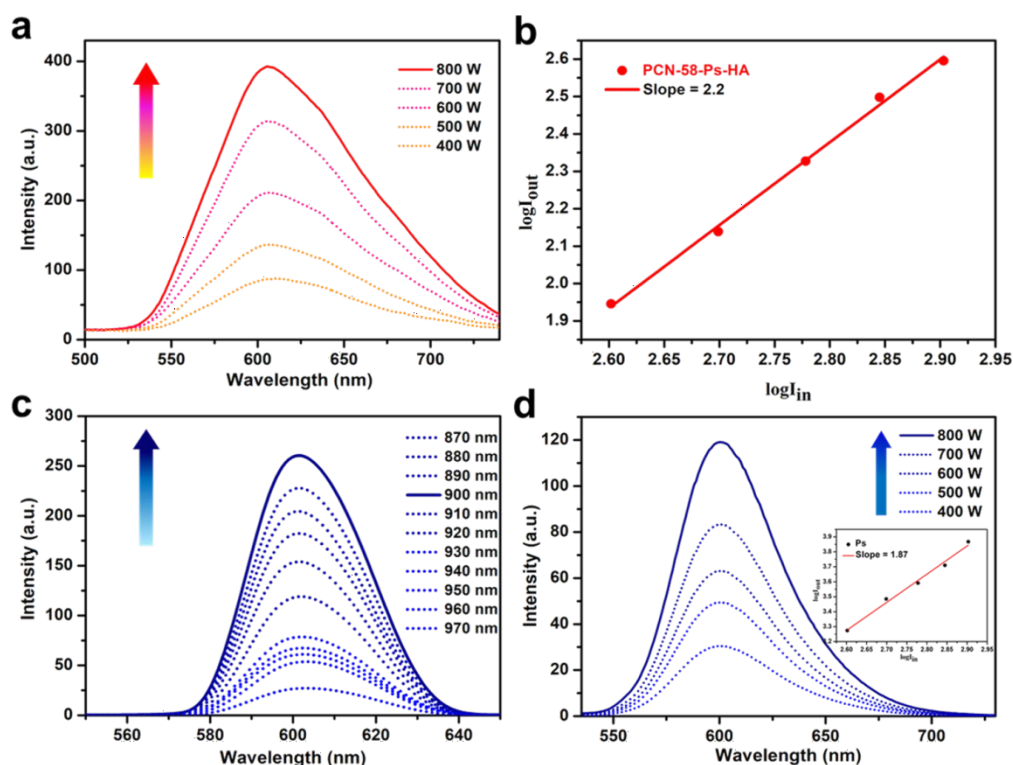


Figure S14 a) Two-photon excited luminescence of **PCN-58-Ps-HA** with femtosecond laser excitation at 910 nm with different input power. b) Two-photon absorption verification of **PCN-58-Ps-HA**. c) Two-photon fluorescence spectra of **Ps** (excited wavelength: 870 nm - 970 nm, 500 mW). d) Two-photon excited luminescence of **Ps** with femtosecond laser excitation at 900 nm with different input power. (Inset: two-photon absorption verification of **Ps**).

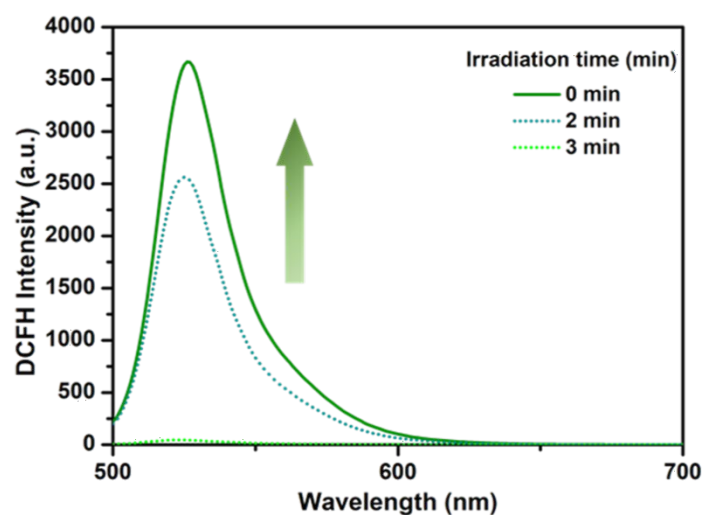


Figure S15 Emission spectra of **PCN-58-Ps-HA** in the solution of DCFH under laser irradiation with different time.

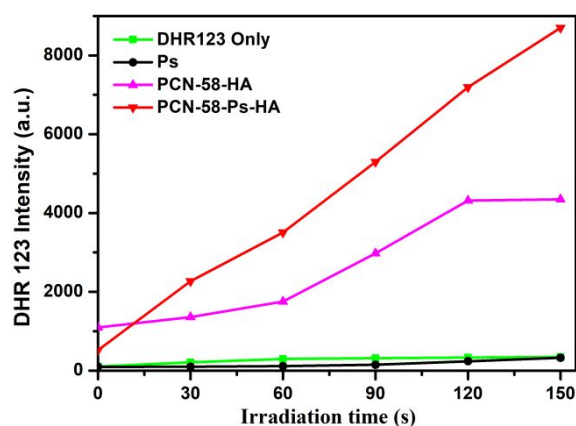


Figure S16 The fluorescence intensity of DHR123 at 525 nm after the LED light (400 - 700 nm, 40 mW/cm²) irradiation for 150s in DHR123 Only, **Ps**, **PCN-58-HA** and **PCN-58-Ps-HA** solution. In contrast to the negligible changes of **Ps**, the evidently enhanced emission of DHR 123 sensitized by **PCN-58-HA** and **PCN-58-Ps-HA** confirmed the light-induced O₂^{•-} generation ability of **PCN-58**.

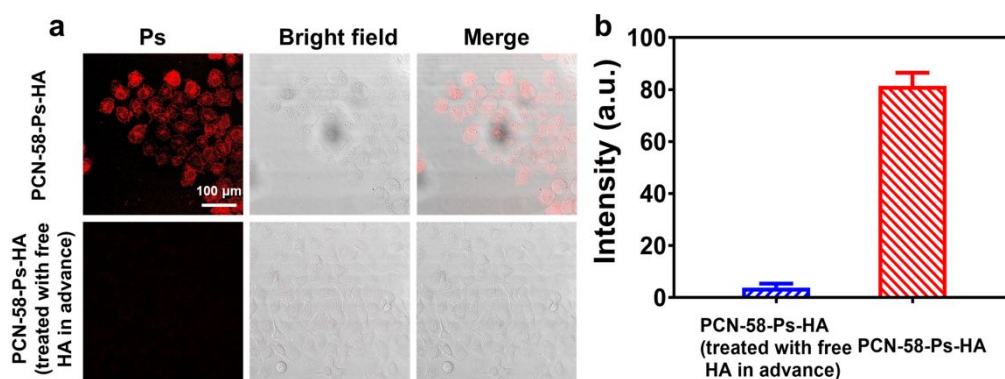


Figure S17 a) CLSM images of HeLa cells incubated with **PCN-58-Ps-HA** (50 µg/mL) and control group (**PCN-58-Ps-HA** treated with free HA in advance). b) Quantitative detection of intracellular fluorescence intensity of **PCN-58-Ps-HA**.

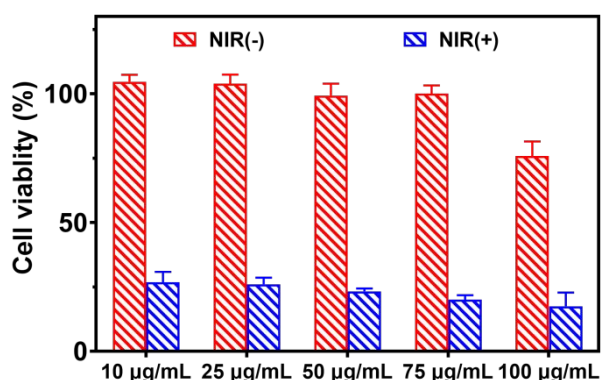


Figure S18 Cell viability of HepG2 cells treated with **PCN-58-Ps-HA** at different concentration with (blue) and without (red) NIR, indicating the good biocompatibility of **PCN-58-Ps-HA** at even high concentration.

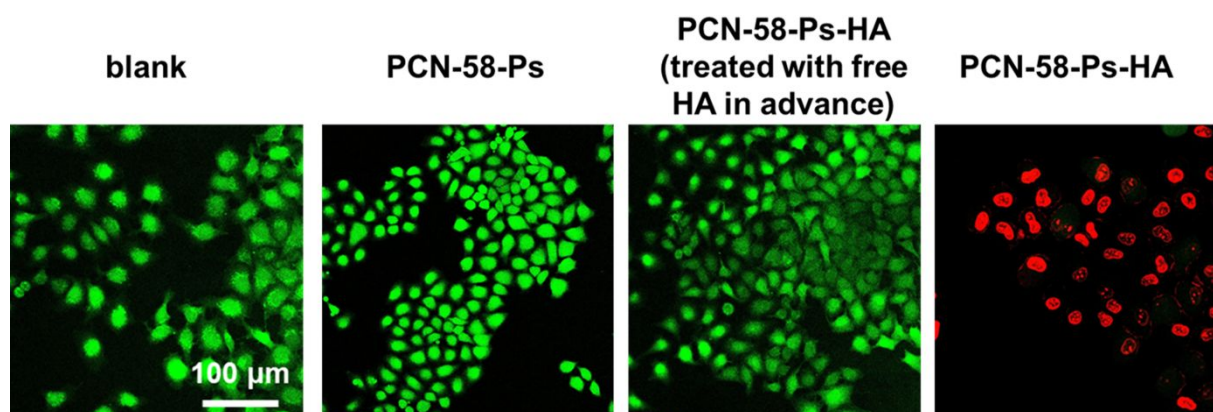


Figure S19 CLSM images of HeLa cells after different treatments and then irradiated for 30 min, stained with calcein AM/PI (910 nm, 0.2 W/cm²).

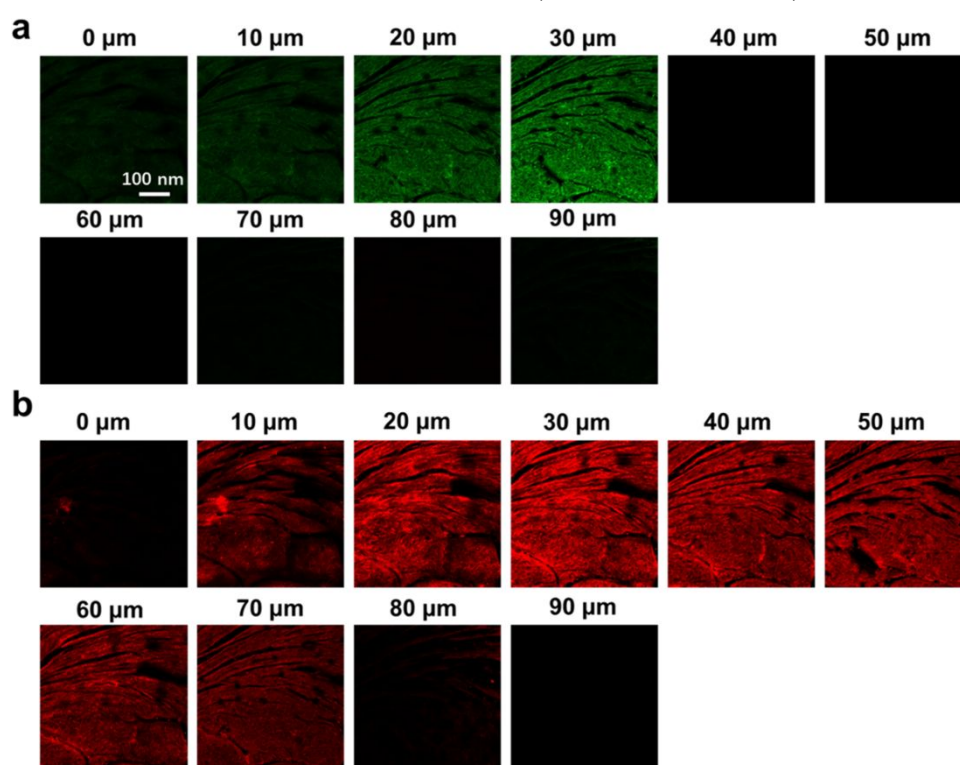


Figure S20 a) One-photon (561 nm, 0.2 W/cm²) and b) two-photon (910 nm, 0.2 W/cm²) fluorescence images of tissue section incubated with PCN-58-Ps-HA with different penetration depth along the z axis.

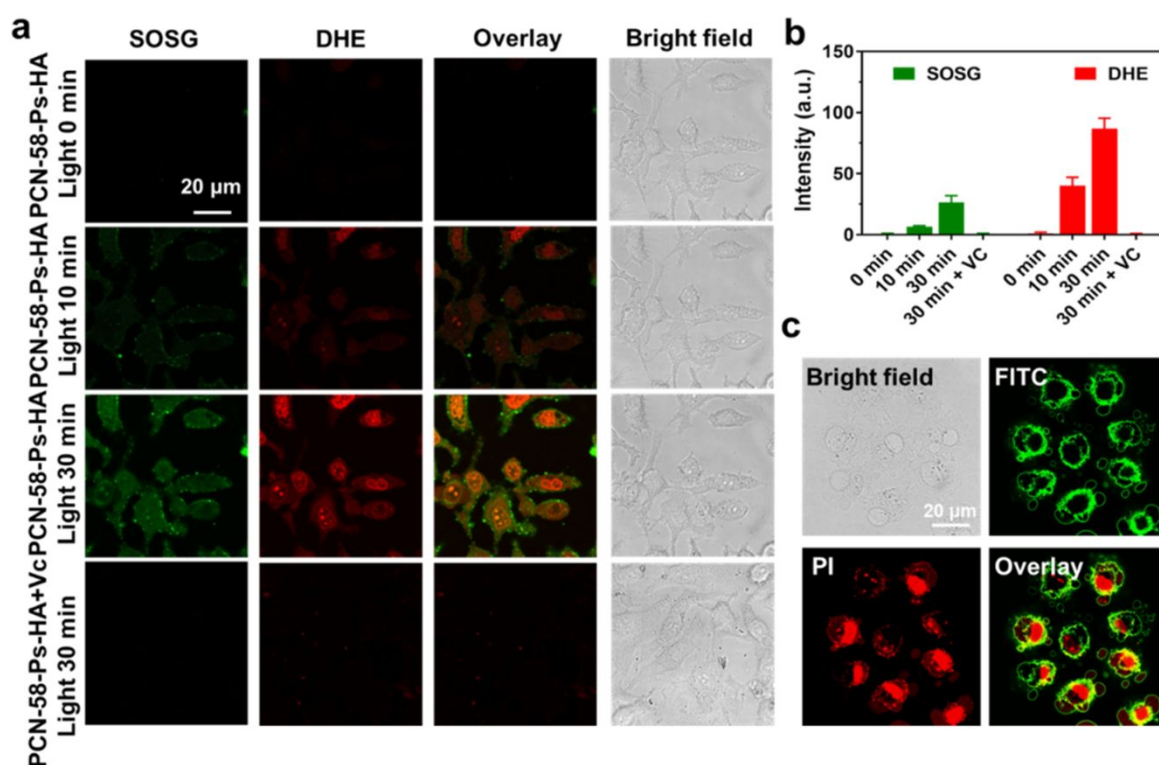


Figure S21 a) Two-photon CLSM images (910 nm, 0.2 W/cm²) of HeLa cells treated with **PCN-58-Ps-HA** and detect the generation of ¹O₂ and O₂^{•-} using SOSG, DHE as the ¹O₂, O₂^{•-} fluorescence indicator, respectively. Victim C, an inhibitor with ROS. b) Fluorescence intensity of SOSG and DHE in HeLa cells treated with **PCN-58-Ps-HA**. c) Annexin V-FITC / PI were indicator of apoptosis.

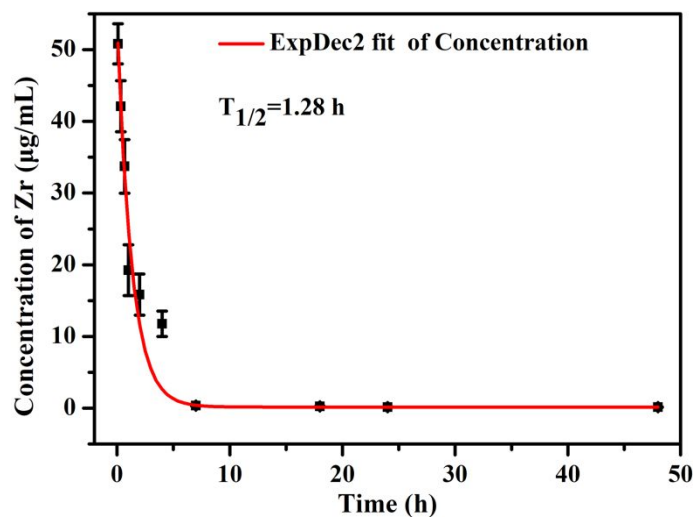


Figure S22 Blood circulation curve of **PCN-58-Ps-HA** determined by measuring the Zr concentration at different time points after injection.

Table S1 Elemental analysis of **PCN-58** and **PCN-58-Ps-HA**.

Name	Content%		
	C	H	N
PCN-58	48.86	3.955	12.17
PCN-58-Ps-HA	48.62	3.546	10.42

Table S2 Zr content in Hela cells determined by ICP-MS

	Concentration of Zr (μg/mL)
PCN-58-Ps	0.14
PCN-58-Ps-HA	100.16
PCN-58-Ps-HA (treated with free HA in advance)	7.46

References

- (1) Zhang, Q.; Lu, X.; Wang, H.; T, X.; Wang, A.; Zhou, H.; Wu, J.; Tian, Y. A benzoic acid terpyridine-based cyclometalated iridium(III) complex as a two-photon fluorescence probe for imaging nuclear histidine. *Chem. Commun.*, **2018**, *54*, 3771-3774.
- (2) Zheng, Z.; Zhang, T.; Liu, H.; Chen, Y.; Kwok, R. T. K.; Ma, C.; Zhang, P.; Sung, H. H. Y.; Williams, I. D.; Lam, J. W. Y.; Wong, K. S.; Tang, B. Z. Bright Near-Infrared Aggregation-Induced Emission Luminogens with Strong Two-Photon Absorption, Excellent Organelle Specificity, and Efficient Photodynamic Therapy Potential. *ACS Nano*, **2018**, *12*, 8145-8159.
- (3) Zheng, X.; Wang, L.; Guan, Y.; Pei, Q.; Jiang, J.; Xie, Z. Integration of metal-organic framework with a photoactive porous-organic polymer for interface enhanced phototherapy. *Biomaterials*, **2020**, *235*, 119792.
- (4) Yi, S.; Lu, Z.; Zhang, J.; Wang, J.; Xie, Z.; Hou L. Amphiphilic Gemini Iridium(III) Complex as a Mitochondria-Targeted Theranostic Agent for Tumor Imaging and Photodynamic Therapy. *ACS Appl. Mater. Interfaces*, **2019**, *11*, 15276-15289.
- (5) Li, M.; Xia, J.; Tian, R.; Wang, J.; Fan, J.; Du, J.; Long, S.; Song, X.; Foley, J. W.; Peng, X. Near-Infrared Light-Initiated Molecular Superoxide Radical Generator: Rejuvenating Photodynamic Therapy against Hypoxic Tumors. *J. Am. Chem. Soc.*, **2018**, *140*, 14851-14859.
- (6) Xu, C., Liu, H., Li, D., Su, J.-H. and Jiang, H.-L. Direct evidence of charge separation in a metal-organic framework: efficient and selective photocatalytic oxidative coupling of amines via charge and energy transfer. *Chem. Sci.*, **2018**, *9*, 3152-3158.
- (7) Karges, J.; Basu, U.; Blacque, O.; Chao, H.; Gasser, G. Polymeric Encapsulation of Novel Homoleptic Bis(dipyrrinato) Zinc(II) Complexes with Long Lifetimes for Applications as Photodynamic Therapy Photosensitisers. *Angew. Chem. Int. Ed.*, **2019**, *58*, 14334-14340.
- (8) Kim, K.; Lee, S. M.; Jin, E. J.; Palanikumar, L.; Lee, J. H.; Kim, J. C.; Nam, J. S.; Jana, B.; Kwon, T. H.; Kwak, S. K.; Choe, W. Y.; Ryu, J. H. MOF × Biopolymer: Collaborative Combination of Metal–Organic Framework and Biopolymer for Advanced Anticancer Therapy. *ACS Appl. Mater. Interfaces*, **2019**, *11*, 27512-27520.
- (9) Wang, B.; Dai, Y.; Kong, Y.; Du, W.; Ni, H.; Zhao, H.; Sun, Z.; Shen, Q.; Li, M.; Fan, Q. Tumor Microenvironment-Responsive Fe(III)-Porphyrin Nanotheranostics for Tumor Imaging and Targeted Chemodynamic-Photodynamic Therapy. *ACS Appl. Mater. Interfaces*, **2020**, *12*, 53634-53645.
- (10) Dong, Y.; Dong, S.; Wang, Z.; Feng, L.; Sun, Q.; Chen, G.; He, F.; Liu, S.; Li, W.; Yang, P. Multimode Imaging-Guided Photothermal/Chemodynamic Synergistic Therapy Nanoagent with a Tumor Microenvironment Responded Effect. *ACS Appl. Mater. Interfaces*, **2020**, *12*, 52479-52491.

- (11) Sang, Y.; Cao, F.; Li, W.; Zhang, L.; You, Y.; Deng, D.; Dong, K.; Ren, J.; Qu, X. Bioinspired Construction of a Nanozyme-Based H₂O₂ Homeostasis Disruptor for Intensive Chemodynamic Therapy. *J. Am. Chem. Soc.*, **2020**, *142*, 5177-5183.
- (12) Lin, H.; Gao, S.; Dai, C.; Chen, Y.; Shi, J. A Two-Dimensional Biodegradable Niobium Carbide (MXene) for Photothermal Tumor Eradication in NIR-I and NIR-II Biowindows. *J. Am. Chem. Soc.*, **2017**, *139*, 16235-16247.
- (13) Meldal, M.; Christian W. T. Cu-Catalyzed Azide-Alkyne Cycloaddition. *Chem. Rev.*, **2008**, *108*, 2952-3015.
- (14) Cohen, S. M.; Wang, Z. Postsynthetic modification of metal-organic frameworks. *Chem. Soc. Rev.*, **2009**, *38*, 1315-1329.
- (15) Hein, J. E.; Fokin, V. V. Copper-catalyzed azide-alkyne cycloaddition (CuAAC) and beyond: new reactivity of copper(I) acetylides. *Chem. Soc. Rev.*, **2010**, *39*, 1302-1315.
- (16) Jiang, H. L.; Feng, D.; Liu, T.; Li, J.; Zhou, H. C. Pore Surface Engineering with Controlled Loadings of Functional Groups via Click Chemistry in Highly Stable Metal-Organic Frameworks. *J. Am. Chem. Soc.*, **2012**, *134*, 14690-14693.